

CEBAF Program Advisory Committee Six (PAC6) Proposal Cover Sheet

This proposal must be received by close of business on April 5, 1993 at:

CEBAF

User Liaison Office

12000 Jefferson Avenue

Newport News, VA 23606

Proposal Title

Separation of $(e, e'\pi)$ Response Functions
versus Q^2 and A

Contact Person

Name: Garth Huber

Institution: University of Regina, Department of Physics

Address: 3737 Wascana Parkway

Address:

City, State ZIP/Country: Regina, SK S4S-0A2 Canada

Phone: (306) 585-4240 **FAX:** (306) 585-4894

E-Mail → BITnet: **Internet:** huberg@meena.cc.uregina.ca

**If this proposal is based on a previously submitted proposal or
letter-of-intent, give the number, title and date:**

Proposal# 89-035, October 30, 1989.

Measuring the Number of Pions in the Nucleus

CEBAF Use Only

Receipt Date: 4/5/93 Log Number Assigned: PR 93-046

By: gh

Research Proposal to CEBAF PAC6

1993 April 5

Separation of $(e, e'\pi)$ Response Functions versus Q^2 and A

A Hall A Collaboration Charter Experiment

Spokesmen:

G.M. Huber, University of Regina (huberg@meena.cc.uregina.ca)

C.C. Chang, University of Maryland (chang@enp.umd.edu)

R. Gilman, Rutgers University (gilman@ruthep.rutgers.edu)

Participants:

G.M. Huber, G.J. Lolos

University of Regina

C.C. Chang, B. Beise, H. Breuer, N.S. Chant, J.J. Kelly, P. Markowitz, P.G. Roos

University of Maryland

R. Gilman, E. Brash, C. Glashauser, G. Kumbartzki, R. Ransome, P.M. Rutt

Rutgers University

E. Cisbani, S. Frullani, F. Garibaldi, M. Jodice, G.M. Urciuoli

INFN-Sanita

J. LeRose, P.E. Ulmer

CEBAF

J. Calarco

University of New Hampshire

M. Manley

Kent State University

Z. Papandreou

George Washington University

Abstract

Pioneering measurements performed with low duty factor beams have demonstrated that studies with the $(e, e'\pi^+)$ reaction promise access to much exciting physics. We propose to perform a survey of the $(e, e'\pi^+)$ reaction versus A and Q^2 using the high resolution spectrometers in Hall A.

The exchange of pions by nucleons inside the nucleus creates a population of constituent pions. The spectral function of this population can be measured via $(e, e'\pi)$ using quasi-free kinematics with excitation above the resonance region. Performing a longitudinal-transverse separation helps to distinguish constituent pion knockout from pion creation on the nucleon. A systematic study using Rosenbluth separations will establish the sensitivity of the reaction to the pionic content of the nucleus, and studies of the cross section versus momentum transfer will probe the dependence of any enhancement or suppression of virtual-pion momentum.

Studies at relatively high values of Q^2 can investigate the propagation of pions through the nuclear medium. One of the predictions of pQCD is that, at large momentum transfer, elastic and inelastic final-state interactions of the hadrons in the nuclear medium will be reduced and that they will exhibit “color transparency”. By performing response function separations for several different Q^2 and A , we aim to obtain data that will allow the extraction of this information in as model-independent way as possible. Measurements at $z \approx 1$ will greatly simplify the interpretation of any data obtained.

Results are presented to indicate that the $(e, e'\pi^+)$ reaction is a superior probe for these studies than many other reactions. Furthermore, many of the sources of systematic error common to L/T separations with these other reactions are shown to be much more easily controlled in $(e, e'\pi^+)$, making this experiment an excellent choice for the early experimental program of Hall A.

Introduction

Much effort has been expended in recent years to study the spin-isospin ($\sigma\tau$) response functions of nuclei, and by implication, the underlying mesonic degrees of freedom. These studies are largely motivated by the target mass dependence of quark structure functions obtained in deep-inelastic scattering [1]. This celebrated EMC effect indicates that some constituents of nuclear matter behave quite differently in a large nucleus than in a free nucleon.

Transverse $\sigma \times \hat{q}$ response functions have been known for some time from backward electron scattering, where they are the most experimentally accessible. The longitudinal $\sigma \cdot \hat{q}$ response function, however, can only be determined from hadronic reactions, such as (\vec{p}, \vec{p}') , or semi-hadronic reactions, such as $(e, e'\pi)$. The hadronic pion exchange force manifests itself in the longitudinal channel, while rho exchange is dominant in the transverse channel at intermediate energies. Thus, a measurement of the longitudinal response has been interpreted as a direct measure of the charge distribution of the nuclear pion field.

There has been an expectation that this nuclear pion field is modified compared to that in a free nucleon. Friman, Pandharipande, and Wiringa [2] have calculated the pion excess in nuclei which results from the exchange of pions by bound nucleons. Berger and Coester [3] explain the EMC effect as an increase in the density of sea quarks in nuclei associated with this pion excess. Akulinichev [4] explains the anomalously large K^+ -Nucleus scattering data [5] by invoking the contribution of the virtual nuclear pion field. However, Frankfurt, Strikman and Liuti [6] point out that any quantitative description of the EMC effect must also take into account the enhanced nuclear valence-quark and gluon distributions, and Miller [7] argues that virtual pion enhancements are not sufficient to explain the K^+ scattering data. Bertsch et al. [8] go so far as to state that there is “a net depletion” of virtual pions within the nucleus. More precise data on the enhancement or suppression of the virtual pion field within the nucleus will be a tremendous aid in resolving this long-standing issue.

A LAMPF measurement [9], performed on various nuclei for inclusive quasi-free proton scattering to isolate the longitudinal response function, which couples directly to the nuclear virtual pion field, did not find any enhancement. However, the interpretation of these results [10] is complicated by the fact that proton distortions restrict the sensitivity of this measurement almost exclusively to the nuclear surface, where density effects are expected to be small, as well as the fact that the inclusive (\vec{p}, \vec{p}') reaction allows contributions from both the isoscalar and isovector channels, which dilutes any expected enhancement. A more recent inclusive (\vec{p}, \vec{n}) measurement at LAMPF [11] is sensitive to only the isovector channel, and has also found no evidence of enhancement. An exclusive $(\vec{p}, \vec{p}'p)$ measurement underway

at IUCF [12] will eliminate the ambiguity due to $(p, 2p)$ and (p, pn) final states, and has sufficient resolution to identify the shell of the struck nucleon, so that the sensitivity to the nuclear interior may be improved. However, hadronic probes have a number of intrinsic limitations. They have difficulty sampling deep inside the nucleus, where any medium effects may be maximal, and the longitudinal and transverse response functions R_L , R_T must be extracted from the polarization transfer observables in a model dependent way [13]. In these respects, studies performed with electron beams have a number of advantages.

While only the spin-independent (charge) longitudinal response is obtainable via quasi-elastic electron scattering [14], recent extractions of it have caused much excitement, indicating that nucleon properties may indeed be modified by the nuclear environment [15, 16, 17]. The measurements of the $(e, e'\pi)$ reaction proposed here will be particularly valuable for the study of the nuclear spin-isospin response. The pion exchange force manifests itself only in the longitudinal spin-isospin channel, and in the transverse channel the particle-hole force is repulsive. Thus, one can expect a net contrast between these two responses for momentum transfer between 2 and 3 m_π . The reduced role of distortions in $(e, e'\pi)$ compared to proton scattering reactions will make the interpretation of these results less ambiguous. Indeed, the kinematic flexibility of the $(e, e'\pi)$ reaction, allowing both response functions to be measured simultaneously, and the good understanding of the elementary process compared to hadronic reactions, make $(e, e'\pi)$ the preeminent tool for studies of the nuclear spin-isospin response [18].

The $(e, e'\pi^+)$ reaction has only been measured so far on deuterium [19] and hydrogen. The deuteron measurements were performed for quasi-free kinematics using the 645 MeV electron beam at Saclay. The electron-scattering angle was 36° and the coincident pions were measured at 34° . Only two photon-nucleon invariant mass settings were obtained, $W = 1160$ and 1232 MeV. For the previous measurements on hydrogen, the longitudinal cross section, which is dominated by quasi-free scattering off virtual pions, is more than twice the transverse cross section at 1160 MeV. At 1232 MeV, the amplitude for Δ production is enhanced. In both cases, the extent to which the basic quasifree-nucleon reaction is modified by the deuteron binding was examined. Even though the deuteron is only loosely bound, Gilman et al. [19] found that the deuteron cross section was quenched by 20% compared to the value for a free proton in the same kinematics. There is speculation that this quenching may signal significant nuclear medium effects.

This pioneering measurement has demonstrated that studies with the $(e, e'\pi^+)$ reaction hold promise for much exciting physics. A systematic study using Rosenbluth separations will be necessary to establish quantitatively the sensitivity of the reaction to the pionic content

of the nucleus. Studies of the cross section versus momentum transfer will be necessary to probe the dependence of any enhancement or suppression of virtual-pion momentum. Studies at relatively high values of Q^2 will be useful for studies of pion transmission through the nuclear medium (color transparency). We propose, in this document, a survey of the $(e, e'\pi^+)$ reaction using the high resolution spectrometers in CEBAF's Hall A, to probe the rich physics much anticipated [20] to be revealed via $(e, e'\pi^+)$.

Measurements at Low Q^2

As discussed above, bound nucleons exchanging pions with their neighbors create a population of virtual pions inside the nucleus, and that the distribution of these pions versus momentum is believed to be different than in a free nucleon. The spectral function of the pions in the nucleus is a theoretically calculable, and an experimentally measureable quantity. Various calculations [2, 3, 21] of the pion density give, for medium weight nuclei, one exchange pion present at any time for every eight nucleons, and that this density is nuclear mass dependent.

The spectral function of the number of pions per nucleon in a nucleus is given by

$$S_\pi(p, E) = \langle \Psi | a_\pi^\dagger a_\pi | \Psi \rangle / A,$$

where Ψ is the nuclear ground state wave function and $a_\pi^\dagger a_\pi$ is the number operator for a pion of momentum p and total energy E . The density due to exchange pions is obtained by subtracting the contribution of the pion cloud around a free nucleon ψ ,

$$\rho_\pi(p, E) = S_\pi(p, E) - \langle \psi | a_\pi^\dagger a_\pi | \psi \rangle. \quad (1)$$

The total number of these exchange (or constituent nuclear) pions is then

$$N_\pi = \int \rho_\pi(p, E) d^3p dE. \quad (2)$$

A calculation of these quantities has been made in reference [2], in which a Hamiltonian for the πNN and $\pi N\Delta$ interactions are used in a variational calculation for $\rho_\pi(p, E)$. Figure 1 shows a plot of the momentum density, and the table below gives the numbers of constituent pions in this model as a function of atomic weight.

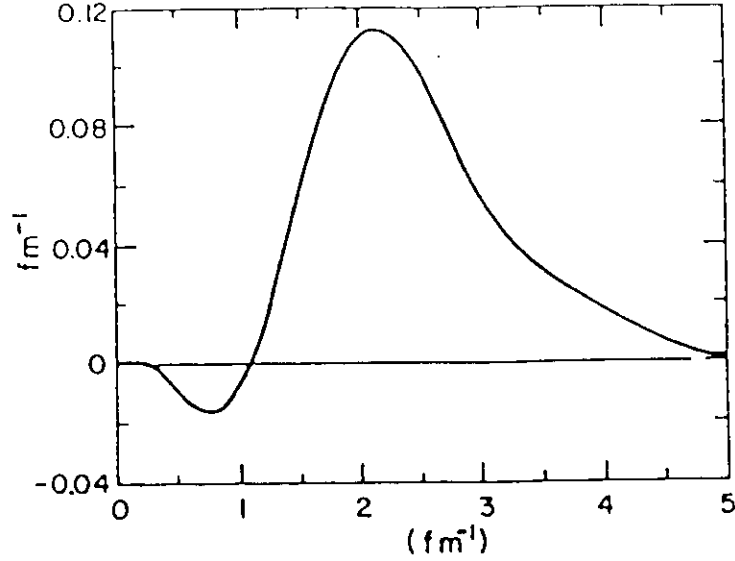


Figure 1. The function $4\pi p^2 \int \rho_\pi(p, E) dE$ versus p from reference [2]. This plot shows the momentum spectrum of constituent pions for a nucleus with a Fermi momentum of 1.33 fm^{-1} .

Number of Constituent Pions per Nucleon [2]	
A	N_π
2	0.024
4	0.09
27	0.11
56	0.12
208	0.14

In reference [21], similar conclusions are reached by a different technique. The pion spectral function is computed from the response function, $R(p, E)$, derived from the pion-nucleus optical potential,

$$S_\pi(p, E) = \frac{1}{\pi} \frac{\text{Im} R(p, E)}{(E + E_0)^2},$$

where E_0 is the on-shell pion energy for momentum p . Figure 2 shows the spectral function associated with the MSU pion-nucleus optical potential [22].

A third theoretical approach to the pion momentum distribution is pursued in reference

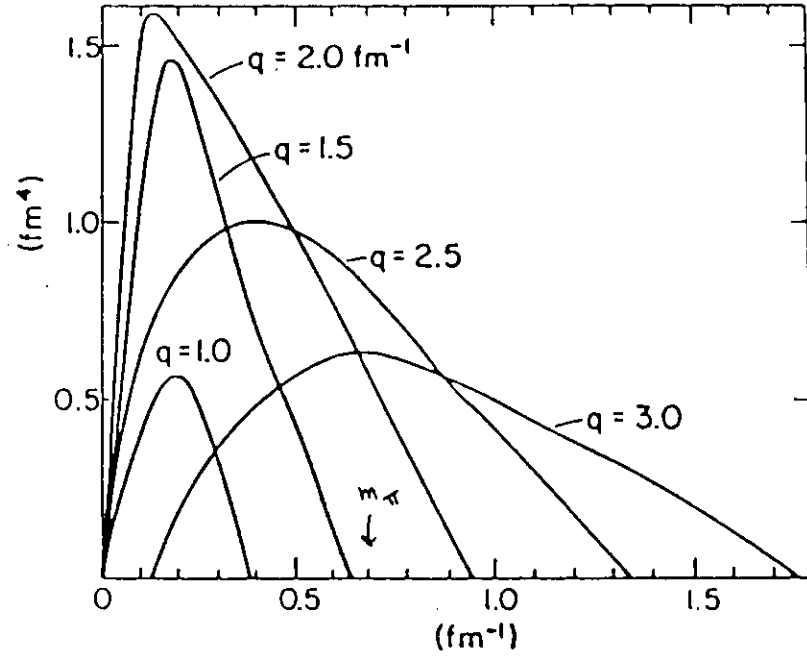


Figure 2. The function $4\pi p^2 \rho_\pi(p, E)$ versus E from reference [21]. This plot shows the energy spectrum of the constituent pions for various values of the pion momentum (here called q) in the nuclear ground state, $N_\pi \approx 0.13$.

[3], where the one pion exchange potential is used directly.

$$\rho(p, E) = -\frac{1}{A} \langle \Psi | \frac{V_{ope}(p)}{E} | \Psi \rangle$$

The conclusions are similar to those of references [2] and [21]. Thus, a measurement of $(e, e'\pi)$ cross sections would allow us to check the connection of the constituent pion spectral function to other fundamental nuclear quantities: the πNN and $\pi N\Delta$ vertex functions, the pion-nucleus optical potentials, and the NN pion exchange potential.

Experimentally, the spectral function of these constituent pions will be measured with the reaction $A(e, e'\pi^+)$ in quasifree kinematics. The pions will be detected near the direction of the three-momentum transfer to the nucleus, and the pion energy will be very near the energy loss of the scattered electron. The analysis philosophy is similar to that used to extracting the bound nucleon spectral function from $(e, e'N)$ measurements. The experiment will be performed in the excitation energy region above the nucleon resonances, and at low four-momentum transfer, Q^2 . These kinematic variables are chosen so that the pion production contribution from nucleon resonances and from hadronizing quarks would be minimized. A longitudinal/transverse separation will be performed to isolate the pion pole term, which should dominate the longitudinal cross section, and to further minimize the contribution of pion production on the nucleon via the Δ resonance, which is mainly a transverse process.

Since the longitudinal cross section is related to the pion spectral function by

$$\frac{d^4\sigma_L(q, \nu, \theta_{e'}, p_\pi, \theta_{\pi q})}{d\Omega_e d\nu d\Omega_\pi dp_\pi} = \sigma_M p_\pi E_\pi f_\pi^2(Q^2) S_\pi(p, E),$$

a measurement of the longitudinal cross section can be easily translated into $S_\pi(p, E)$, the pion spectral function, in the quasi-free approximation. In the equation above, σ_M is the Mott cross section, p_π and E_π are the momentum and total energy of the detected pion, and $f_\pi(Q^2)$ is the form factor of the pion. In this approximation, the initial momentum, p , and energy, E , of the pion are given by the missing momentum and missing energy

$$p_m = |\vec{q} - \vec{p}_\pi| \quad E_m = \nu - E_\pi.$$

Essentially the same technique has been used by Guttner et al. [24] to determine the pion distribution function of the proton. Using longitudinal π^+ electroproduction data on hydrogen at $Q^2 = 0.70 \text{ GeV}^2/c^2$ and $W = 2.19 \text{ GeV}$, they determined that the physical proton has a 3% $n\pi^+$ state admixture, and that this π^+ carries 0.6 % of the proton momentum. Similar results on the nucleus should generate considerably more interest.

It is obvious from Equations (1) and (2) that it is necessary to measure the two-dimensional spectral function over a wide range of original pion momentum p and energy E . An estimate of these ranges can be estimated from the theoretical predictions, as shown in Figures 1 and 2. They are:

$$\begin{aligned} \text{range of } p: & 0 \rightarrow 1.0\text{GeV}/c \\ \text{range of } E: & 0 \rightarrow 0.3\text{GeV}. \end{aligned}$$

Our proposed kinematic settings will be discussed in more detail in a later section.

Measurements at High Q^2

One of the questions at the interface between particle and nuclear physics is the topic of Color Transparency (CT), a prediction of perturbative QCD (pQCD) applied to the nuclear medium. QCD has the important simplifying feature that at high Q^2 there is asymptotic freedom [23]. This implies that the magnitude of the strong coupling constant should diminish as Q^2 increases, and permits the use of perturbation theory in QCD calculations. One prediction of pQCD is that, at large momentum transfer, the elastic and inelastic final-state interactions of the hadrons in the nuclear medium will be reduced [25, 26].

As a consequence of perturbative QCD, the spatial extent of the quark separations in the struck system is argued to be of order $1/Q$. Thus, in high Q^2 pion electroproduction, there are reasons to believe that the pion must have diminished transverse size (or be a so-called "mini-hadron"), and so will have a smaller interaction with the surrounding nucleons. This can be understood in a simple color Van-der-Waals model for the strong interaction, where a smaller size implies a smaller color dipole moment, and a smaller interaction strength. This novel effect, that nuclear matter may be anomalously transparent to hadrons at large momentum transfer, was predicted independently by Mueller [26] and Brodsky [25], and is called "color transparency".

Recent measurements in quasielastic $(p, 2p)$ scattering at Brookhaven [27] have observed an energy dependence to the nuclear transparency, defined as

$$T(Q^2, A) = \frac{1}{Z} \frac{d\sigma/dt(p, A \rightarrow pp(A-1))_{90^\circ}}{d\sigma/dt(pp \rightarrow pp)_{90^\circ}}$$

as shown in Figure 3. This figure shows that both the high-energy pp elastic scattering cross sections and the transparency ratio exhibit large oscillations with energy. The oscillations

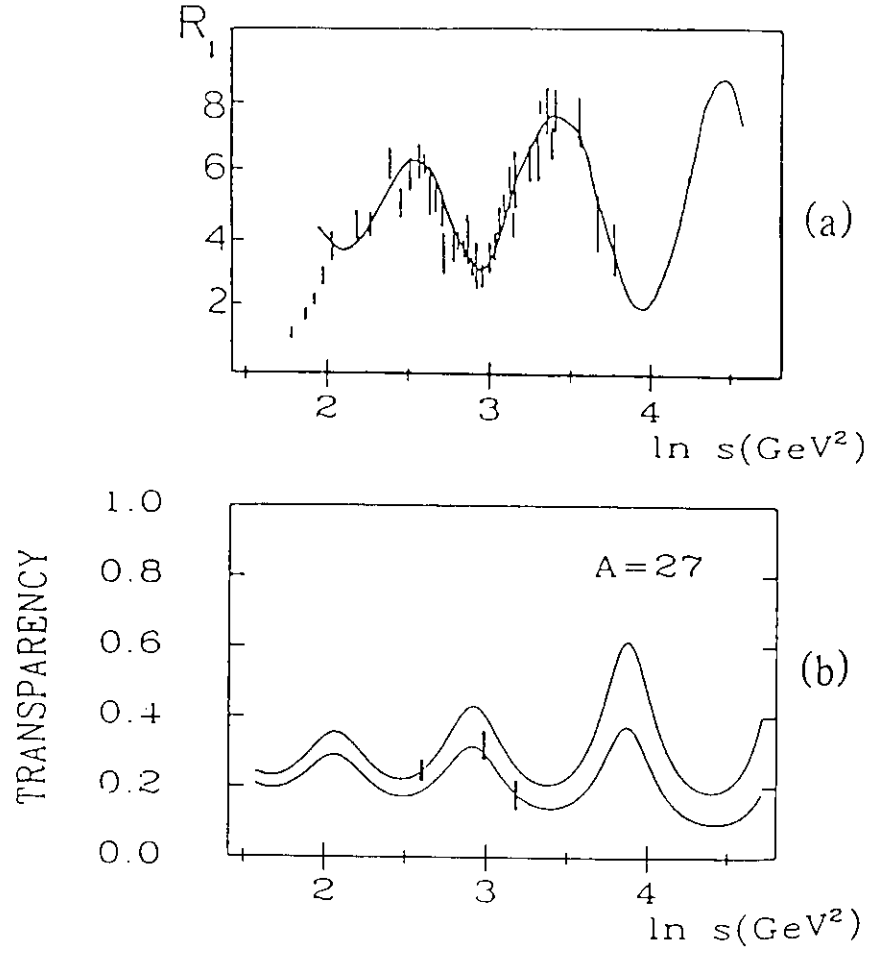


Figure 3. (a) The energy dependence of $R_1(s) = \text{const} \times s^{10} d\sigma/dt(pp \rightarrow pp)_{90^\circ}$ for high energy pp elastic scattering at 90° c.m. angle. (b) Transparency ratio data on $^{27}\text{Al}(p, 2p)$ [27] as well as predictions by Ralston and Pire [29].

in the 90° elastic pp scattering cross sections indicate interference among several competing amplitudes in the reaction mechanism. Dividing the nuclear cross sections by the pp cross section leads to the oscillations in the extracted transparency ratio, which has been a real problem for the theoretical analysis of this result. By including long ($\approx 1fm$) interaction contributions due to high mass dibaryon resonances [28], or Landshoff contributions [29, 30] in the theoretical models, these oscillations have been reproduced with varying success. Jennings and Miller [31] have investigated the idea that the energy dependence of the transparency is due to an interference between the two different effects.

A new method of analyzing this data has recently been proposed by Jain and Ralston [32], which is claimed to be considerably less model dependent than the transparency ratio method. The new data analysis method allows both the hard scattering rate inside the nuclear medium and the attenuation rate of the struck system to be extracted empirically. By fitting the shape of the A dependence of the cross section at fixed momentum transfer with the attenuation cross section $\sigma_{eff}(Q^2)$, as well as the normalization $N(Q^2)$, as free parameters, they deduce a survival probability for hadrons propagating through the nucleus. Figure 4 shows the proton survival probability extracted from their fit to the $(p, 2p)$ data as a function of Q^2 . The rise in the survival probability with Q^2 is offered as evidence of color transparency, and it coincides with predictions based on the attenuation cross section scaling as the transverse separation of the participating quarks. This new analysis technique holds much promise for the future identification of subtle CT effects.

High $Q^2 < 7GeV^2/c^2$ measurements of quasielastic $(e, e'p)$ scattering from nuclei have been recently completed by the NE18 collaboration [33] at SLAC. Quasielastic proton knockout with an electron probe is intrinsically clean because of the known electromagnetic interaction, and the absence of oscillations in the basic cross section. However, the theory of hard scattering form factors is controversial, and there are reasons to believe that at laboratory values of momentum transfer there may be non-short-distance contributions to the free space nucleon form factors [34]. If nuclear filtering is correct, then some of these contributions should be filtered away in a large nuclear target - for example, in the case of the pion form factor, there is a prediction that normalization of the $1/Q^2$ dependence may be closer to the asymptotic QCD result for $A \gg 1$ [32]. It follows that in the SLAC experiment, one must determine the hard scattering rate in the nuclear target before interpreting the transparency ratio. The meaning of preliminary results showing observation of a flat Q^2 dependent transparency ratio is not yet clear until the full data set is analyzed. In general, good statistics over a range of A and Q^2 are needed; by using all of the data, the determination of color transparency is well defined.

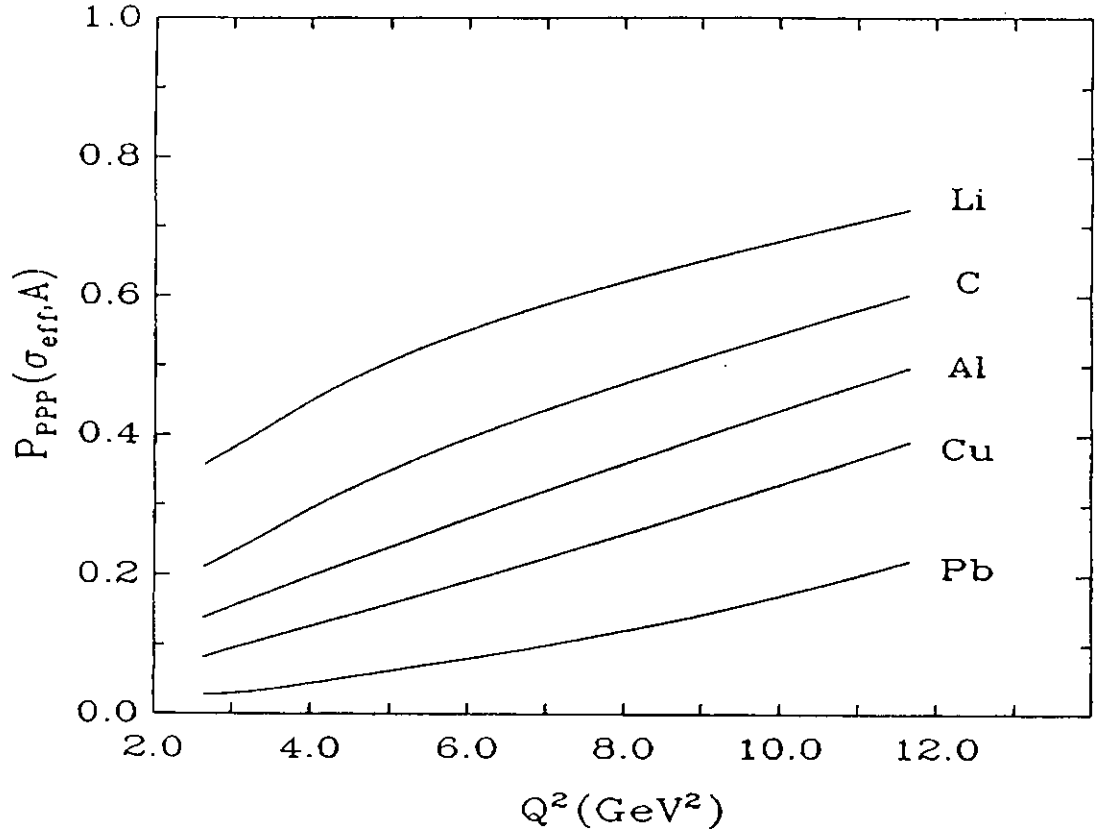


Figure 4. The proton survival probability P_{ppp} extracted by Jain and Ralston [32] from the data of Carroll et al. [27] as a function of Q^2 for various A .

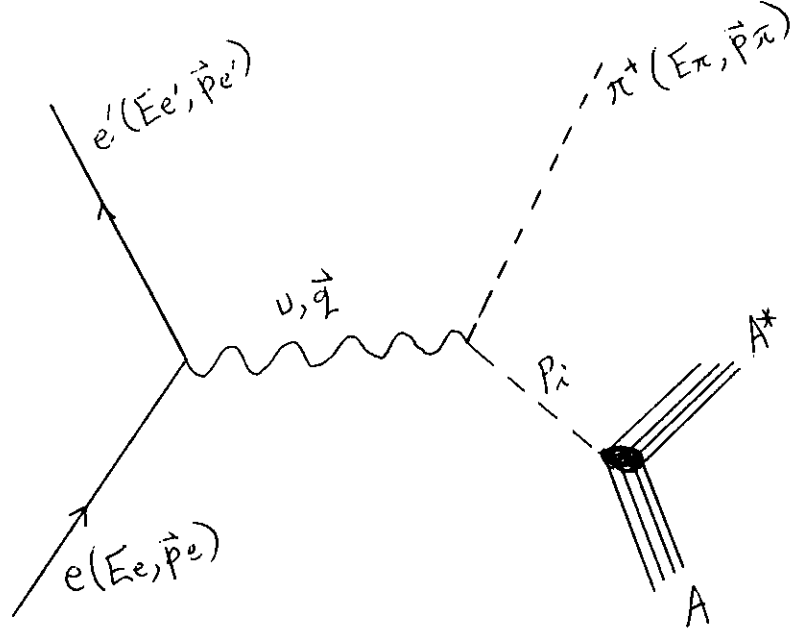


Figure 5. Kinematics of the electroproduction of pions for the reaction $A(e, e' \pi^+) A^*$ in the laboratory system.

Pion electroproduction is expected to provide an exciting test of the color transparency prediction. Comparing CT effects between pions and protons could be illuminating, as the difference between the two must be sensitive to the quark-bag dynamics while each entity is in the mini-hadron state. If it is possible to isolate the appropriate production mechanism, the pion is likely to be a better testing ground than the proton for transparency ideas. As will be discussed below, there is some expectation that the longitudinal channel will exhibit a larger CT effect than the transverse channel, so a separation of the longitudinal from the transverse response function will cleanly isolate the production channel expected to be most sensitive to CT effects.

The kinematics of the $(e, e' \pi)$ reaction are shown in Figure 5. In the case of pions, the

form factor in free space is known to obey the simple counting rule

$$F_\pi(Q^2) \propto \alpha_s(Q^2)/Q^2,$$

which makes it much larger at large momentum transfer than the nucleon form factor. As long as p_1^2 is not far from the pion pole, $(e, e'\pi)$ reactions on a nucleus may be described in terms of this form factor. This feature should make it easier to investigate transparency predictions with pion production than with proton knockout. With limited statistics, a pion electroproduction experiment can determine some combination of the hard scattering rate versus the attenuation cross section. With good statistics, however, the effective attenuation cross section and the hard scattering rate can be more easily separated. The object is to knock a virtual pion on-shell, and observe the difference in its interaction with the nucleus as it travels its way outwards, versus Q^2 and A .

Rationale Behind the High Q^2 Kinematics

The only high Q^2 L/T separation that has been attempted on $(e, e'\pi^+)$ was performed on hydrogen by Bebek et al. [35] in 1977, as a test of Feynman scaling predicted by the quark-parton model. A portion of their data is displayed in figure 6.

The invariant structure function $F = (E/\sigma_t) \frac{d\sigma}{dp_\pi}$ is plotted as a function of the Feynman scaling variable x' (or x_F), the ratio of the pion's longitudinal momentum to its maximum possible longitudinal momentum in the center-of-momentum frame. Near $x' = 1$, x' is approximately equal to z , the fraction of the electron's energy loss, ν , that is carried by the ejectile pion. For $x' < 0.7$, the distributions can be seen to be rather smooth, decreasing exponentially with increasing x' , and exhibiting approximate Feynman scaling in that the data depend upon x' , but not upon Q^2 or W . This scaling is predicted by the parton model, and indicates a process in which the virtual photon is absorbed on a single quark, which then hadronizes. Investigations in this region are aimed at studying the hadron formation length that occurs, due to color confinement, when a quark undergoes a hard process in deep inelastic electron scattering on nuclei. This effect is expected to increase the attenuation cross section as Q^2 increases, causing an interplay of CT and formation zone effects [36]. As the cross section for this type of interaction decreases approximately as $(1 - z)^n$, little contribution is expected as $z \rightarrow 1$.

In figure 6, the cross section increases again when $x' > 0.7$. This is due primarily to the exclusive reactions $p(e, e'\pi^+)n$ ($x' \approx 1$) and $p(e, e'\pi^+)\Delta^0$ ($x' \approx 0.85$). In contrast to the low x' region, here the hadronization process is prompt, and the pion emerges with all of the

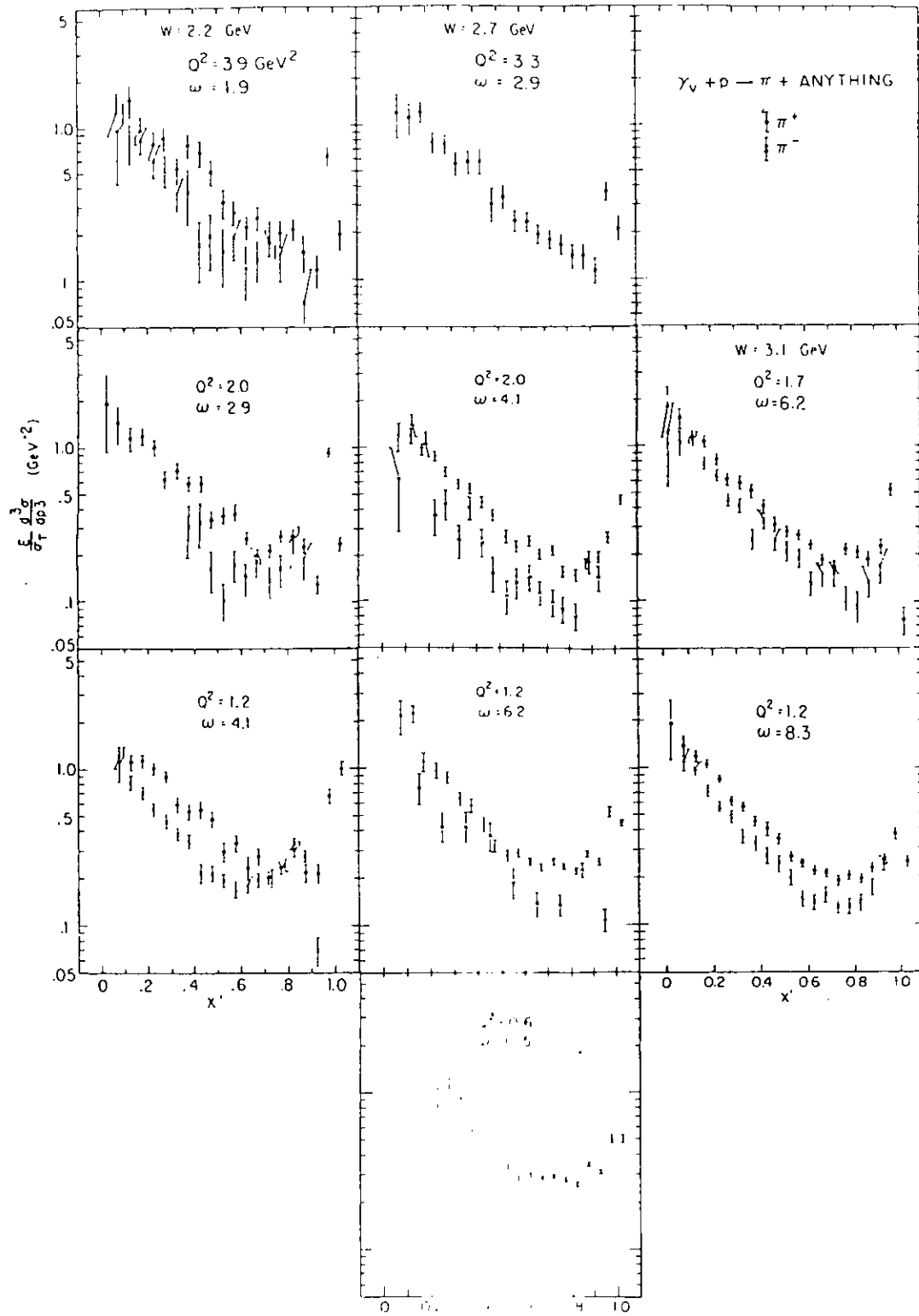


Figure 6. $p(e, e' \pi^+)$ structure functions for $p_T = 0.02 \text{ GeV}^2/c^2$ from reference [35].

available energy, leaving behind the struck nucleon in either the ground or Δ state. The high x' data does not exhibit Feynman scaling, and especially for pions emitted in parallel kinematics, the cross section decreases relatively quickly with increasing Q^2 . It is consistent with the knockout of a virtual pion from the struck nucleon. Thus, at intermediate values of z one addresses issues related to the propagation of individual quarks through nuclear matter, and as $z \rightarrow 1$, one begins to learn about the possible transparency effects of the nucleus to color-neutral hadrons.

The difference in the pion production mechanism between high and low z corresponds to the longitudinal and transverse components of the cross section. The longitudinal component is strongly peaked towards forward kinematics, corresponding to $t \approx 0$, or $z \approx 1$; this is shown in figure 7. The transverse cross section is largest away from the photon direction, and dies off near $t \approx 0$. Compelling arguments have been advanced that the longitudinal cross section arises from a direct coupling to the pion current. For example, in contrast to the sharp forward-peaking seen in π^+ photoproduction, no comparable peaking occurs in π^0 production, presumably due to the inability of the photon to couple directly to the π^0 meson exchange current. On the other hand, the transverse response is dominated by isobar resonance and hadronization mechanisms. Since quarks have spin 1/2, they can only absorb transverse virtual photons due to helicity conservation. This is consistent with experimental results in deep inelastic scattering, where the measured L/T ratio is very small. The finite value of the ratio comes from higher twist (virtual parton loop) contributions, or the non-zero primordial transverse momentum of quarks in the nucleon.

The issues of a L/T separation and measurements at high z are, in our opinion, intertwined. Performing the measurements at $z \approx 1$ greatly simplifies the interpretation of any data obtained. At high Q^2 , there may be concern about the applicability of a L/T separation when there are many newly-created particles in the final state. This, however, is indicative of a multi-particle hadronization (i.e. transverse) process, and is severely restrained by our choice of high z kinematics. This is particularly true of nearly exclusive one pion production, and is a distinct advantage in this case over proton knockout. Similarly, difficulties in interpretation due to the role of higher energy pion resonances are also minimized by the L/T separation.

The separated L and T response functions may also exhibit different CT characteristics. The pions observed in the longitudinal channel are knocked-out directly in a high Q^2 interaction, and so should be most sensitive to any CT effect. The major mechanism in the $(e, e'\pi^+)$ transverse channel at high energy is the hadronization process; at somewhat lower energy, pion production via the Δ dominates. In both of these processes, the pions observed are not

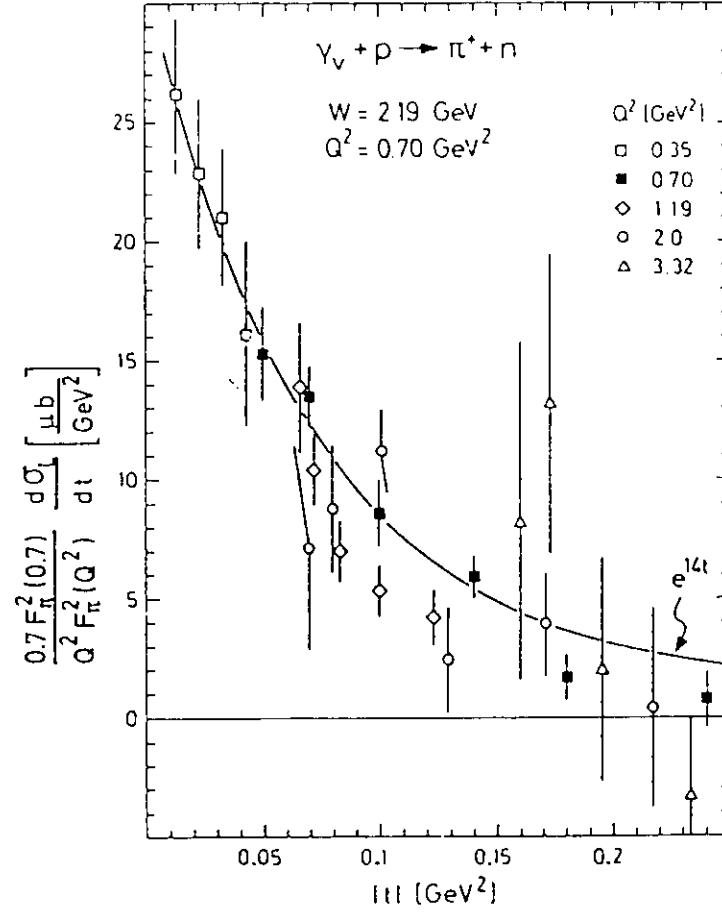


Figure 7. $\gamma_v + p \rightarrow \pi^+ + n$ longitudinal cross sections from reference [37]. Data have been scaled in Q^2 .

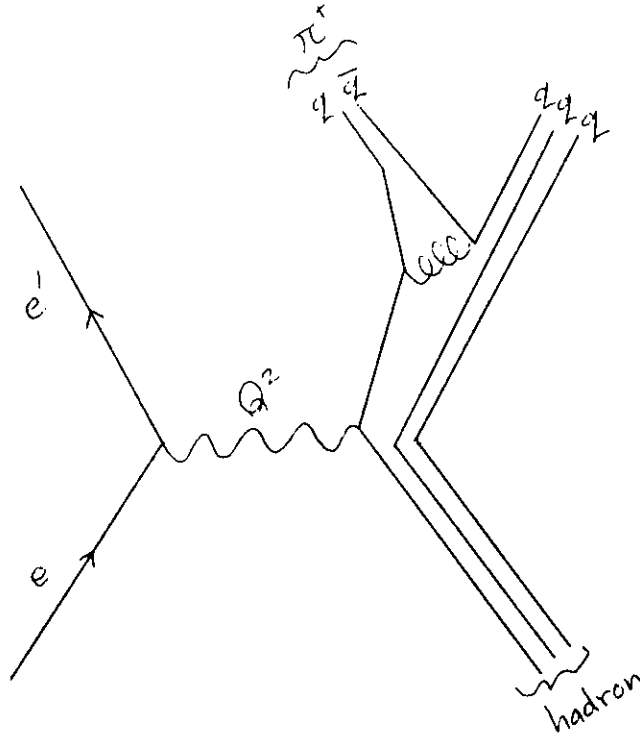


Figure 8. Higher twist contribution to single meson production. The first high Q^2 interaction is between the virtual photon and a quark within the nucleon. This quark emits a gluon, which turns into a quark-antiquark pair. One quark is re-absorbed by the nucleon, while the antiquark combines with the “original” quark to form a pion.

produced directly from a high Q^2 process, and so the CT signal should be diluted. However, a higher twist mechanism, shown schematically in figure 8, could produce a CT effect in the transverse channel. Because of the high virtuality at the gluon vertex, the effective Q^2 observed by the pion could be large, and the pion could be produced as a mini-hadron. In the case that different CT effects are observed in the two channels, this would be a very interesting result. Thus, a L/T separation is crucial for any study of pion electroproduction at higher Q^2 .

These arguments indicate that a pion electroproduction color transparency measurement must be made at a very large value of z (i.e. one pion carrying essentially all of the energy transfer), and that it is necessary to either perform the measurements in a region where the L component dominates ($t \approx 0$), or to perform a L/T separation at each value of Q^2 . In order to maximize the longitudinal component of the cross section, the absolute value of t is to be kept as small as possible. Since it is not possible to keep $|t| < 0.05 \text{ GeV}^2/c^2$, where the longitudinal cross section is at least four times the transverse cross section for all values

of Q^2 desired, it will be necessary to perform Rosenbluth separations at each of the values of Q^2 proposed here (0.58, 2.0, and $3.5 \text{ GeV}^2/c^2$). These measurements would be performed on six target nuclei across the periodic table, $p, d, {}^4\text{He}, {}^9\text{Be}, {}^{27}\text{Al}$, and ${}^{107}\text{Ag}$.

The greatest value of Q^2 proposed here, $3.5 \text{ GeV}^2/c^2$, is the highest that can be practicably investigated with 6 GeV beam at CEBAF. Figure 9 shows a variety of different predictions for the Q^2 dependence of the transparency ratio for $(e, e'\pi)$ on Argon at high $z > 0.8$. These indicate that significant CT effects should be observable for Q^2 as low as $2 \text{ GeV}^2/c^2$ with $(e, e'\pi)$. This calculation is obviously not meant to be definitive, so we show a similar set of calculations by the same author for $(e, e'p)$. It is the relative sensitivities of the two reactions at the same value of Q^2 , and the relative size of the error bars that we wish to point out here. These plots reinforce our view that a Rosenbluth separation of $(e, e'\pi)$ at large z is superior to $(e, e'p)$ for the study of CT. The results would be a useful probe in the so-called “transition CT” region. Higher Q^2 results, from either SLAC or the proposed EEF, would provide data in the “asymptotic CT” region.

Description of the Experiment

We wish to obtain our measurements using the twin spectrometers in Hall A and cryotargets. We propose to perform L/T separations of the $(e, e'\pi^+)$ reaction at three different values of Q^2 , 0.58, 2.00, and $3.50 \text{ GeV}^2/c^2$, on six target nuclei across the periodic table, $p, d, {}^4\text{He}, {}^9\text{Be}, {}^{27}\text{Al}$, and ${}^{107}\text{Ag}$.

Choice of Kinematics

For an electron with 4-momentum (E_e, \vec{p}_e) scattered into solid angle $\Omega_{e'}$ with 4-momentum $(E_{e'}, \vec{p}_{e'})$, the charged pion electroproduction cross section can be written in terms of a photoproduction cross section by a virtual photon with 4-momentum $(\nu = E_e - E_{e'}, \vec{q} = \vec{p}_e - \vec{p}_{e'})$. It can be shown [41] that the charged-pion electroproduction cross section can be written as

$$d\sigma/d\Omega_\pi dE_\pi d\Omega_{e'} dE_{e'} = \Gamma [d\sigma_T/d\Omega_\pi dE_\pi + \epsilon d\sigma_L/d\Omega_\pi dE_\pi + \epsilon \cos 2\phi d\sigma_{TT}/d\Omega_\pi dE_\pi + \sqrt{2\epsilon(\epsilon+1)} \cos \phi d\sigma_{LT}/d\Omega_\pi dE_\pi]$$

where $d\sigma_T/d\Omega_\pi dE_\pi$ is due to unpolarized transverse photons, $d\sigma_L/d\Omega_\pi dE_\pi$ is due to longitudinal polarized photons, $d\sigma_{TT}/d\Omega_\pi dE_\pi$ is due to the interaction of transverse linearly

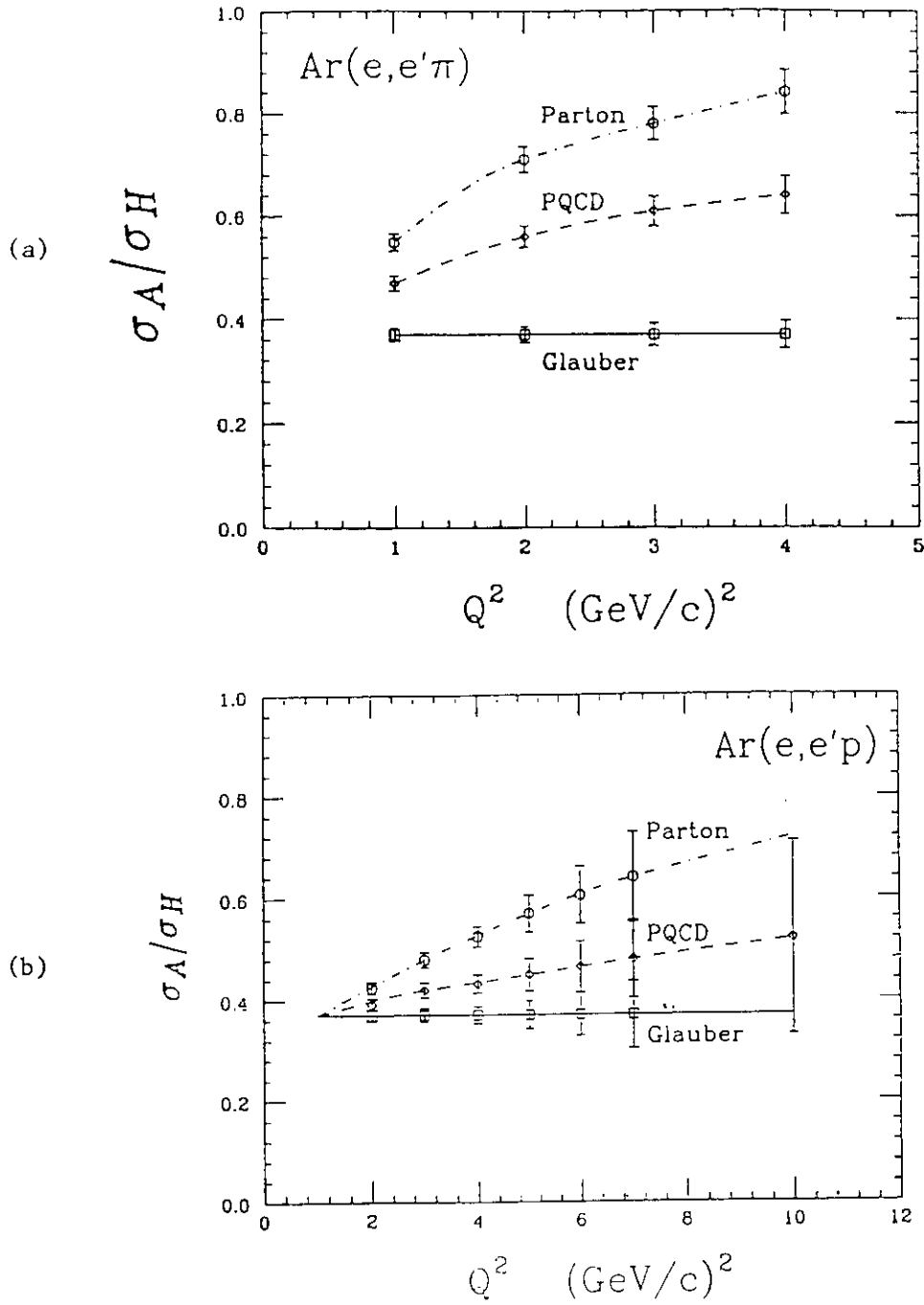


Figure 9. (a) The Q^2 dependence of the transparency ratio σ_a/σ_H for electropion production from an argon target. The curves correspond to three models for nuclear attenuation of the pions. (b) Same for quasi-elastic scattering from protons in an argon target. The data points shown are for the same integrated luminosity at the SLAC NPAS station as in plot (a) [38].

polarized photons, and $d\sigma_{LT}/d\Omega_{\pi}dE_{\pi}$ is due to the interference of transverse and longitudinally polarized photons, and Γ is a kinematic factor.

Since transverse $\sigma \times \hat{q}$ response functions have been known for some time, and $(e, e'\pi)$ is particularly well suited to extracting the elusive longitudinal $\sigma \cdot \hat{q}$ response function, we are largely interested in the longitudinal response function in this proposal. We have chosen a nucleon-pion invariant mass above the resonance region to minimize the number of pions created via Δ resonances by the virtual photon, $W = 2.00\text{GeV}$. The resonant portion of the cross section will be further reduced by separating off the transverse portion.

As discussed previously, measurements over a large missing momentum and energy range are needed in order to determine the two-dimensional pion spectral function. For a given electron kinematics, the missing momentum and energy can be scanned by changing the observed pion momentum p_{π} and its detection angle with respect to the three-momentum transfer vector $\theta_{\pi q}$. As seen in Figure 10, to scan the missing energy one should vary p_{π} while keeping $\theta_{\pi q}$ fixed, and to scan the missing momentum, one should vary $\theta_{\pi q}$ while keeping p_{π} fixed. Thus, to cover the range of missing momentum and energy required, the cross section should be measured over a range of $0 < \theta_{\pi q} < 25^{\circ}$ and $1.0 < P/P_0 < 1.15$. As the acceptance of each HRS^2 spectrometer is 60mr horizontally, 130mr vertically, and $+/- 5\%\delta P/P$, eight settings of the pion angle, and two settings of the pion momentum are required to cover the pion angular and momentum range desired.

By making two measurements at the same $\theta_{\pi q}$ on either side of the \vec{q} vector, only the sign of the out-of-plane angle ϕ is modified, enabling the LT response function to be separated. By taking advantage of the $+/- 3.7^{\circ}$ vertical acceptance of the spectrometer, it may be possible to attempt a separation of the TT response function as well. Figure 11 shows a Monte Carlo simulation of the ϕ acceptance of the HRS^2 spectrometers in $(e, e'\pi)$ coincidence. These separations will be attempted, but it should be noted that they are not the main goal of this proposal.

For the measurement of the pion spectral function, we chose a low value of the four-momentum transfer to avoid suppression of the cross section due to the pion form factor. However, due to the limitation that the smallest central angle setting of each HRS^2 spectrometer is 12.5° , we have chosen an energy loss of 1971 MeV , and a four-momentum transfer of $0.580\text{ GeV}^2/c^2$ for the central kinematic settings. We also intend to make several measurements at small $\theta_{\pi q}$ at the two higher Q^2 in order to determine the momentum transfer dependence of the reaction.

These constraints allow the following range of epsilon to be covered. As the horizontal acceptance of the spectrometer is 3.43° , a spectrometer setting of 12.5° allows horizontal

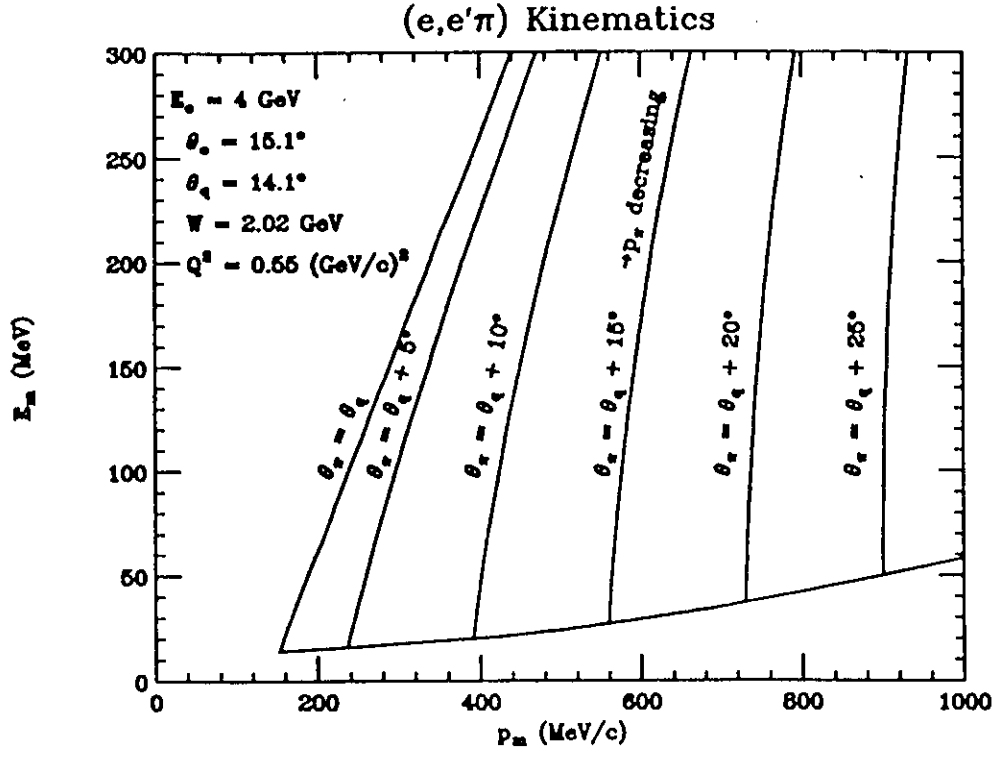


Figure 10. Missing energy, E_m , versus missing momentum, p_m , for the kinematic variables indicated.

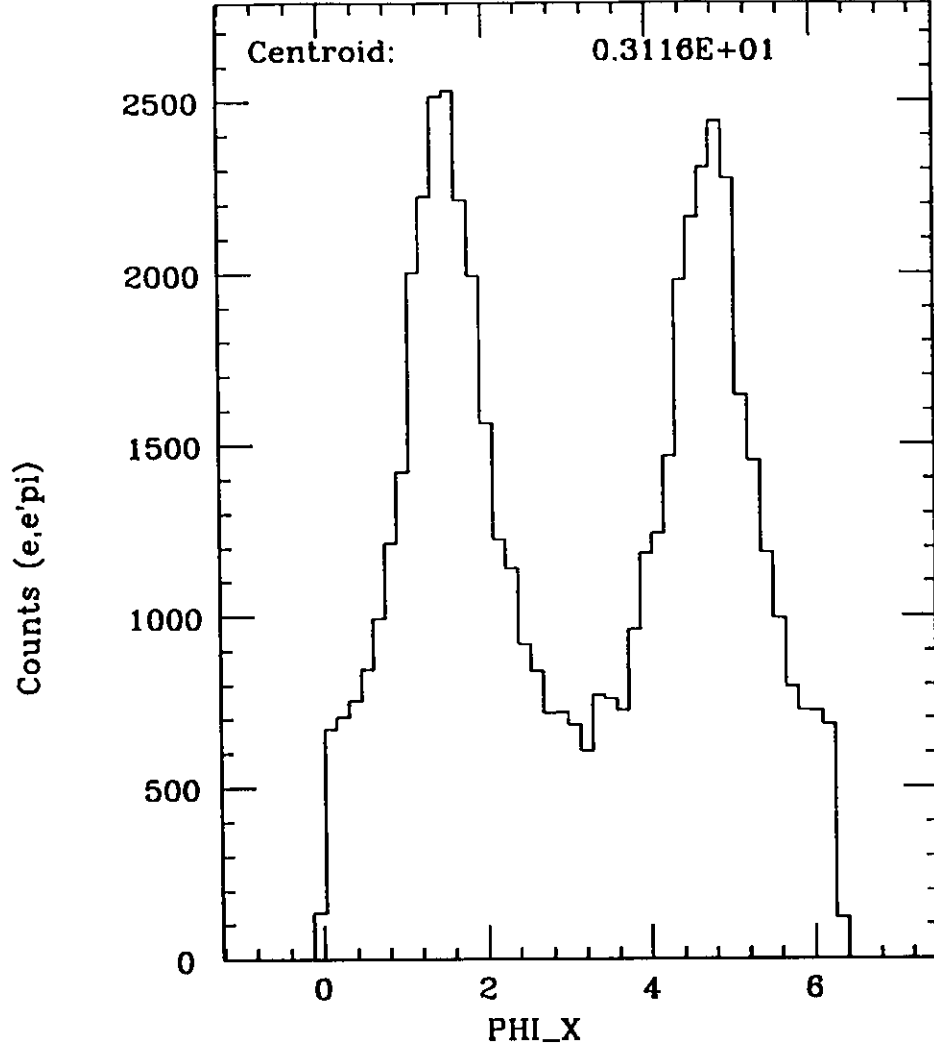


Figure 11. $p(e, e' \pi^+) n$ coincidence yield versus the angle between the electron scattering and hadron production planes ϕ . The x-axis units are in radians. The two peaks correspond to $\phi = 90^\circ$ and $\phi = -90^\circ$ (i.e. production above and below the scattering plane), as the vertical acceptance of each spectrometer is approximately twice the horizontal acceptance.

angles as small as 10.78° to enter the spectrometer. However, to improve the data taking efficiency for small $\theta_{\pi q}$, we only accept central settings which place the three-momentum vector at angles greater than 11.8° . If a beam energy up to only 4.0 GeV is available, then only the first two settings on the table below would be measured. Otherwise, the second setting would be skipped and the third at 4.6 GeV done instead, in order to reduce uncertainties in the L/T separation, as well as completing the remainder of the table.

ϵ	E_e GeV	$E_{e'}$ GeV	$\theta_{e'}$ deg	p_π GeV/c	θ_q deg	Q^2 GeV ² /c ²	W GeV
$\nu = 1.971 \text{ GeV}, q = 2.113 \text{ GeV}/c \text{ with } \theta_{\pi q}, p_\pi \text{ scan}$							
0.569	3.00	1.03	25.02	1.95	-11.89	0.58	2.00
0.781	4.00	2.03	15.36	1.95	-14.74	0.58	2.00
0.843	4.60	2.63	12.57	1.95	-15.71	0.58	2.00
$\nu = 2.728 \text{ GeV}, q = 3.073 \text{ GeV}/c, \text{ no scan}$							
0.463	3.90	1.17	38.63	2.62	-13.77	2.00	2.00
0.802	6.00	3.25	18.48	2.62	-19.56	2.00	2.00
$\nu = 3.570 \text{ GeV}, q = 4.041 \text{ GeV}/c, \text{ no scan}$							
0.337	4.60	1.07	49.85	3.29	-11.83	3.50	2.00
0.637	6.00	2.48	28.08	3.29	-16.97	3.50	2.00

Counting Rate Estimates

The only special requirement of this proposal is the need to have good particle identification in both spectrometers. Thus, this experiment requires the use of the silica aerogel cerenkov counter on the hadron spectrometer, and the gas cerenkov and shower counters on the electron spectrometer. We will see, however, that a number of abilities planned for Hall A, such as high resolution spectrometer tunes, or beam property knowledge to the 10^{-4} level are not required for this proposal.

Our cross section estimates have been based upon the $p(e, e'\pi^+)n$ measurements of Brauel et al. [37], converted to $d^3\sigma/d\Omega_{e'}d\Omega_\pi dP_\pi$ via the formalism summarized by Devenish and Lyth [39]. These π^+ production cross sections were obtained at DESY in 1973 with excellent missing mass resolution, and a full decomposition of the L,T,LT and TT components of the cross section. They covered a range of Q^2 from 0.06 to 1.35, at $W = 2.19\text{GeV}$, at incident electron energies from 2.77 to 6.55 GeV. Thus, they are high quality data near to our kinematics of interest, and are therefore expected to provide reliable count rate estimates for this experiment.

A parameterization of these four $(e, e'\pi^+)$ response functions measured on hydrogen has been included in the MCEEP Monte Carlo code of Ulmer [40] as an aid for the planning of this proposal. The rates and cross sections listed in the table on the next page were obtained via the Monte Carlo, averaged over the acceptance of the two spectrometers. The rates are for a luminosity of 1.3×10^{38} , which corresponds to $50\mu A$ current on a 700 mg/cm^2 H_2 cryogenic target (density 70 mg/cm^3 with spectrometer longitudinal acceptance of 10 cm). The high momentum bites at 3.0 GeV and 4.6 GeV are not listed in this table. All quantities are self explanatory, except $\eta_{\pi s}$, which is the mean pion survival fraction through the hadron spectrometer. Counting rates shown have been corrected for pion decay by this factor.

We wish to emphasize that the cross sections and rates listed in the following table are for the $p(e, e'\pi^+)n$ reaction, where a missing mass cut about the neutron mass has been used to eliminate events where the neutron is left in an excited state, such as the Δ^0 . The $z \approx 1$ nucleon-pion events are the main interest of this proposal. However, due to the large momentum acceptance of the spectrometers, some fraction of delta-pion events will be obtained simultaneously, which will be analyzed separately. No estimate of the rate from this reaction has been attempted here.

In estimating our measurements on various nuclei, we have assumed that the quasi-free production cross section scales as Z compared to the free cross section on hydrogen, which should be a conservative estimate. Due to the Fermi momentum smearing, the rate from quasi-free pion production on a bound nucleon should be depressed at small $\theta_{\pi q}$ and enhanced at large $\theta_{\pi q}$ relative to the production on a free nucleon.

Cross sections and Rates on Hydrogen							
Q^2 GeV^2/c^2	E_e GeV	p_π GeV/c	$\theta_{\pi q}$ deg	$d^3\sigma$ $pb/MeV/sr^2$	$\eta_{\pi s}$	Events/hr	Time hr
0.58	3.00	1.951	0.610	3.15	0.80	5769	5
0.58	3.00	1.942	3.844	2.64	0.80	4828	5
0.58	3.00	1.915	6.935	1.64	0.80	2984	6
0.58	3.00	1.871	10.242	0.89	0.79	1635	7
0.58	3.00	1.813	13.755	0.59	0.78	1084	8
0.58	3.00	1.744	17.213	0.50	0.78	914	8
0.58	3.00	1.660	20.659	0.48	0.77	873	8
0.58	3.00	1.584	24.068	0.47	0.76	850	8
0.58	4.60	1.942	-3.800	15.8	0.80	52760	1
0.58	4.60	1.951	0.021	18.0	0.80	61092	1
0.58	4.60	1.942	4.310	14.3	0.80	51984	1
0.58	4.60	1.915	7.067	8.47	0.80	32555	2
0.58	4.60	1.871	10.140	4.35	0.79	17438	3
0.58	4.60	1.813	13.585	2.47	0.79	10199	4
0.58	4.60	1.744	17.191	1.85	0.78	7740	4
0.58	4.60	1.660	20.661	1.72	0.77	7329	4
0.58	4.60	1.584	24.079	1.66	0.76	7020	4
2.00	3.90	2.62	0.035	0.28	0.85	575	8
2.00	6.00	2.62	0.026	1.49	0.85	6000	4
3.50	4.60	3.29	0.016	0.09	0.88	167	12
3.50	6.00	3.29	0.056	0.24	0.88	832	6
Beamtime on Hydrogen: 172 Hours							

L/T Separation Method

When the pion is detected in the forward direction (i.e. in the direction of the virtual photon momentum), the charged-pion electroproduction cross section can be cleanly decomposed into transverse and longitudinal pieces. The LT interference and TT polarized transverse response functions disappear, and the linearity in ϵ can be exploited via a Rosenbluth separation to obtain an exact separation between the two spin-isospin response functions.

A model-independent separation can only be performed for those bins which are common to both the high epsilon and low epsilon measurements. In past $(e, e'p)$ L/T separations,

model-independent separations were difficult if not impossible, since the instruments were too poor to determine bins with any resolution. It was, therefore, common to average over the entire acceptance subject to gross cuts to make an approximate phase space match, and then to average over regions excluded by one or the other measurement using a model for the excluded region. The response functions obtained in this way are not true response functions, since they average over different regions of the phase space (that is the two measurements from which they are extracted). In our simulations of $p(e, e'\pi^+)n$ on the HRS^2 , however, the kinematics allow a close match so the separation can be performed bin-by-bin. If there are sufficient statistics, one could simply compare the R_L and R_T so obtained vs. theta with a theoretical model. Otherwise, one must then average over as much of the common region as is needed to obtain reasonable statistics. Of course, the comparison with theory would involve the same averaging procedure.

In order to investigate the role of systematic errors upon the L/T separation, and to demonstrate that the beamtimes listed in the previous section provide adequate statistics for the separation, at least in the $p(e, e'\pi^+)n$ case, we have sorted simulated data from the Monte Carlo into bins versus ϵ , Q^2 and W . As the $(e, e'\pi^+)$ cross section changes fairly slowly and smoothly with momentum and angle, relatively large bins can be used to obtain a reliable L/T separation without spreading the statistics too thinly. In the simulation performed here, bins of width 13.3 MeV in W , $0.027\text{GeV}^2/c^2$ in Q^2 , and .01 in ϵ were used. To test the level of sensitivity to this procedure, a simulation was also run in which the bin sizes in Q^2 and W were halved. This made essentially no change in the separated response functions, except that the statistical error bars were enlarged because the same number of events were now spread over a larger number of bins. As a 13 MeV bin width in $W = 2000\text{MeV}$ is 1 part in 150, the lack of sensitivity to the bin width change indicates that the spectrometer optics need only to be understood to approximately the 1 part in 1000 level at the time of the running of this experiment, as opposed to the ultimate resolution capability of the spectrometers of 1 part in 10000.

Figure 12 shows the extracted $p(e, e'\pi^+)n$ L and T response functions plotted versus Q^2 and W over the coincidence acceptance for the lowest momentum setting at $\theta_{\pi q} = 0$. Figure 13 shows a slice through these distributions, plotted versus Q^2 , and the expected error bars after 5 hours of running at the low epsilon point, and 1 hour of running at the high epsilon point with a luminosity of 1.3×10^{38} . These error bars are representative of the error bars achieved for each bin in W and Q^2 . Figures 14, 15 similarly show slices through the extracted L and T response functions, and expected statistical error bars for the proposed data points at $Q^2 = 2.0, 3.5\text{GeV}^2/c^2$, respectively.

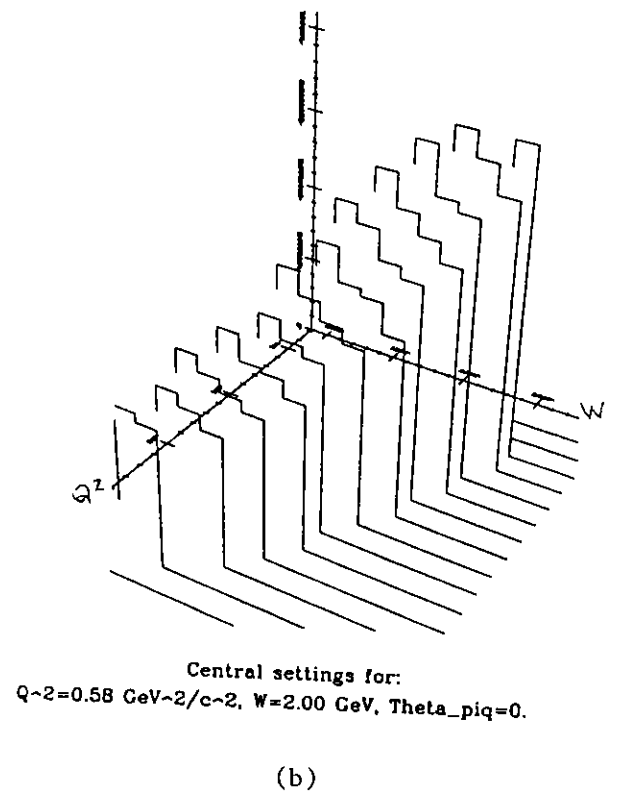
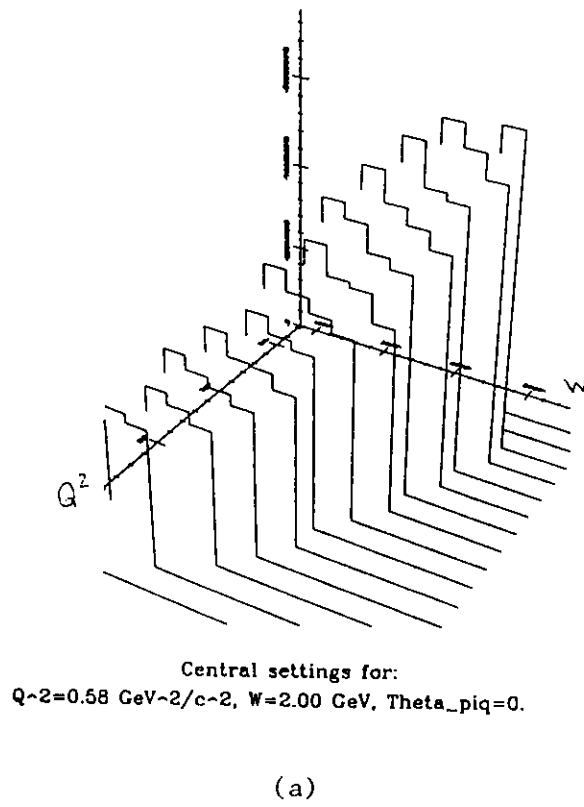


Figure 12. (a,b) $p(e, e'\pi^+)n$ longitudinal and transverse response functions plotted versus Q^2 and W , as simulated for one setting of the HRS^2 spectrometers by MCEEP.

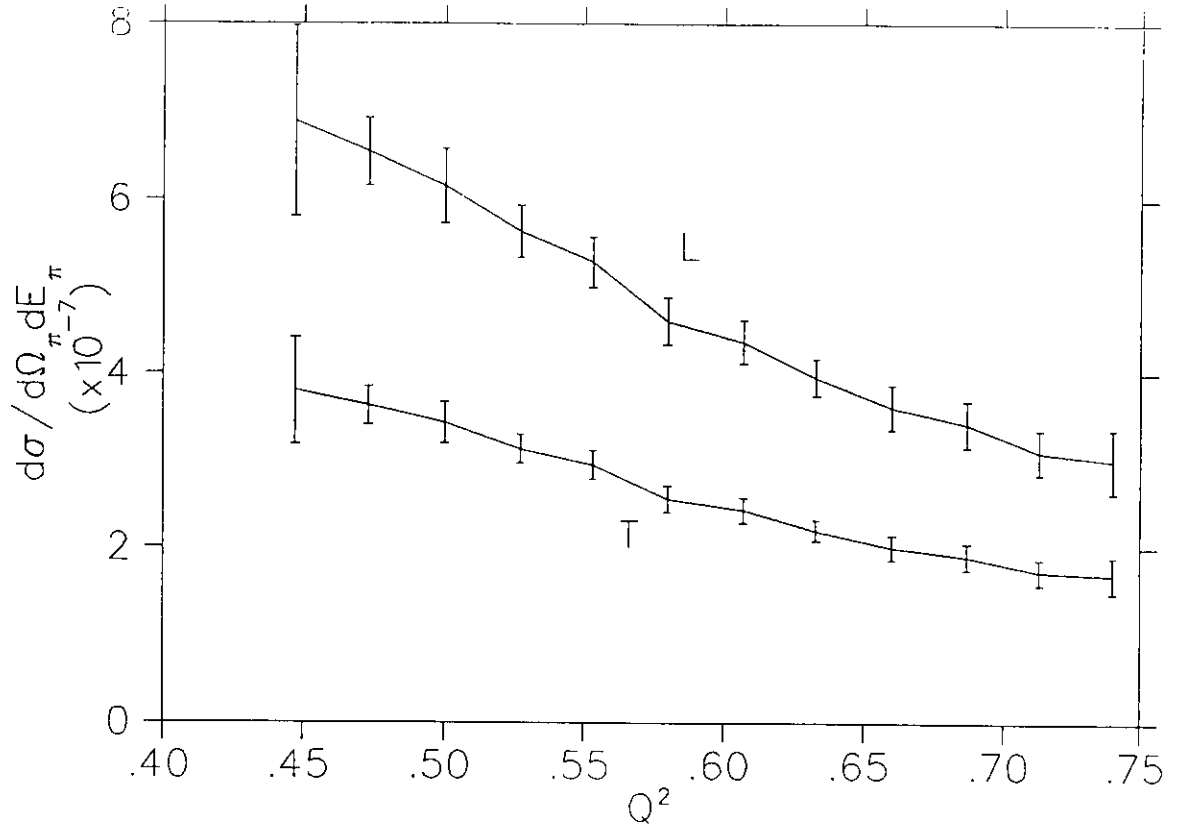


Figure 13. The response functions of figure 12 plotted versus Q^2 for central settings of the HRS^2 of $Q^2 = 0.58 \text{ GeV}^2/c^2$ at $E_e = 3.0, 4.6 \text{ GeV}$, $\nu = 1.971 \text{ GeV}$ and $q = 2.113 \text{ GeV}/c$. The error bars shown are the average error bar for each Q^2 , W bin in figure 12. Statistics were not combined over all W bins in order to improve the statistical accuracy.

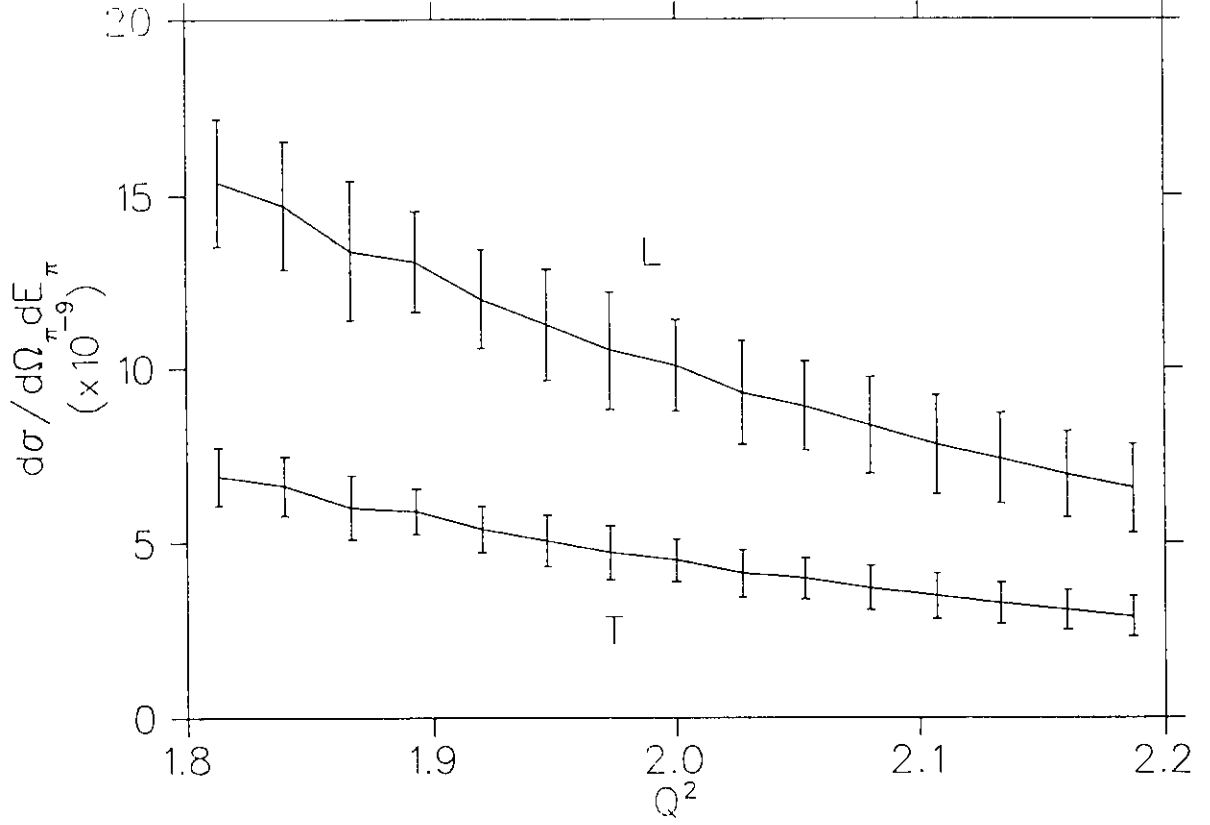


Figure 14. The response functions extracted for central settings of the HRS^2 of $Q^2 = 2.00 \text{ GeV}^2/c^2$ at $E_e = 3.9, 6.0 \text{ GeV}$, $\nu = 2.728 \text{ GeV}$ and $q = 3.073 \text{ GeV}/c$ plotted versus Q^2 . The error bars are as in figure 13.

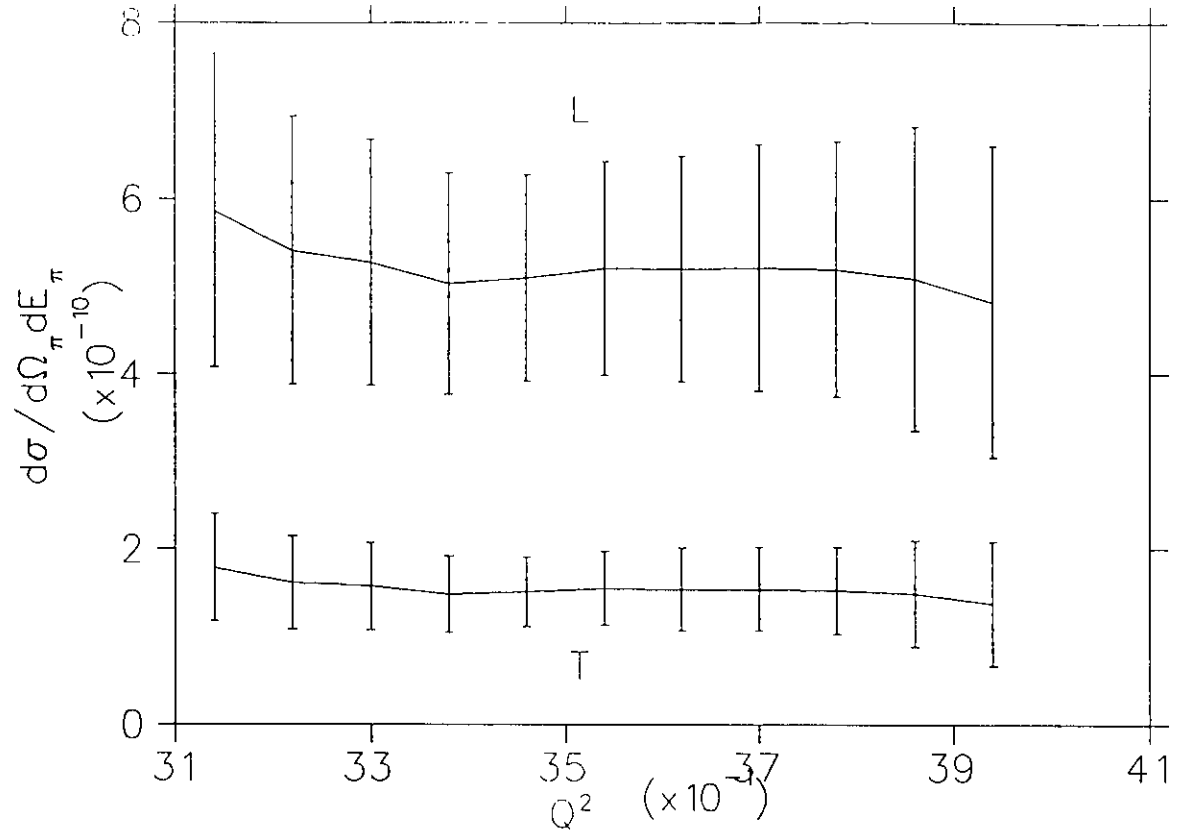


Figure 15. The response functions extracted for central settings of the HRS^2 of $Q^2 = 3.50 \text{ GeV}^2/c^2$ at $E_e = 4.6, 6.0 \text{ GeV}$, $\nu = 3.570 \text{ GeV}$ and $q = 4.041 \text{ GeV}/c$ plotted versus Q^2 . The error bars are as in figure 13.

These results indicate that acceptable L/T separations can be performed for $(e, e'\pi^+)$ reactions within a reasonable beamtime period. We show below that the luminosities required to perform these measurements are well within the specifications for the Hall A instrumentation and target. We should also note that the method of L/T separation performed above demands the most statistical accuracy, but is the least model dependent of the available methods. If statistics prove to be insufficient, we can resort to sorting the data in larger bins, or make a model dependent separation as has been commonplace before.

Sensitivity to Systematic Errors

Sources of systematic error in $(e, e'p)$ L/T separation measurements have been detailed in a CEBAF technical report by Ulmer et al. [42]. This report shows that in order to perform a reliable $(e, e'p)$ response function separation, it is necessary to have a precise understanding of beam position, energy, and stability in order to obtain a reliable separation measurement. As the uncertainty $\delta R_L/R_L$ is approximately

$$\frac{\delta R_L}{R_L} = \left[\frac{\eta}{r\Delta\epsilon} \right] \frac{\delta\sigma_f}{\sigma_f}$$

where $\eta = R_T/R_L$, $r = 2Q^2/\vec{q}^2$ and $\Delta\epsilon = \epsilon_f - \epsilon_b$. At large \vec{q} , there is a large magnification of the uncertainty in R_L relative to the uncertainties in the measured cross sections. At $q = 3\text{GeV}/c$, a 1% uncertainty in the forward angle $(e, e'p)$ cross section translates into a 22% uncertainty in R_L . As the $(e, e'p)$ cross section changes on the order of 1% for each 10^{-4} change in incident electron beam energy, and changes by 1% with each 0.1 *mr* beam angle variation, the beam properties must be known to at least this level of accuracy.

We have studied the sensitivity of the $p(e, e'\pi^+)n$ cross sections to similar types of errors. The table below indicates that the $(e, e'\pi^+)$ reaction is on the order of 1 order of magnitude less sensitive to systematic beam uncertainties than the $(e, e'p)$ reaction, scaling approximately with the ratio of the proton and pion masses. Thus, it should be possible to obtain a reliable $(e, e'\pi^+)$ L/T separation measurement fairly early in the Hall A experimental program, before the beam properties are known to the level necessary to perform $(e, e'p)$ L/T separation measurements.

Sensitivities $\delta\sigma/\sigma$ for $p(e, e'\pi^+)n$					
E_e <i>GeV</i>	Q^2 <i>GeV²/c²</i>	Energy % per $10^{-4}\delta E_0/E_0$	Beam Angle % per mrad θ_b	Scattered E_e' % per $10^{-4}\delta E_e'/E_e'$	Scattered θ_e' % per mrad θ_e'
3.00	0.58	0.14	0.49	0.05	0.46
4.60	0.58	0.20	0.93	0.12	0.91
3.90	2.00	0.29	0.57	0.06	0.57
6.00	2.00	0.34	1.43	0.23	1.43
4.60	3.50	0.10	0.24	0.06	0.24
6.00	3.50	0.11	0.25	0.07	0.25
Sensitivities $\delta\sigma/\sigma$ for $d(e, e'p)n$ (PR-89-026) [42]					
1.7			13.		

Singles and Accidental Rate Estimates

Singles and accidental coincidence rates have been estimated using the code of Lightbody and O'Connell [43], which has been incorporated within MCEEP.

We have chosen luminosities in order to keep the singles rate in the hadron spectrometer (which is expected to observe the highest rate due to the polarity of its magnetic field) below 250 *kHz*. This is a factor of 4 below the design capability of the Hall A instrumentation of approximately 1 *MHz*. These luminosities and singles rates are shown in the table below; singles rates at other spectrometer settings are comparable. For the cryogenic targets, they are based upon the densities listed on page A8-21 of the CDR [44] and a spectrometer longitudinal acceptance of 10 *cm*. As the cross section scales as Z , but the maximum luminosity dictated by the singles rates also scales as $1/Z$, the time required to acquire data for a heavy nuclear target is about the same as that of hydrogen.

Singles Rates at 4.0 <i>GeV</i> (<i>kHz</i>)					
Target	Luminosity	e^-	π^-	p	π^+
p	1.3E38	30	2	35	41
⁴ He	8.0E37	84	24	179	24
²⁷ Al	1.4E37	97	28	189	26
¹⁰⁷ Ag	2.6E36	74	23	133	17

Figure 16 shows a Monte Carlo simulation of the the expected relative TOF between the electron and hadron spectrometers with central momenta of 950 *MeV/c* and 1729 *MeV/c*, respectively. This figure indicates that a relative timing window of 4 *ns* is necessary to acquire

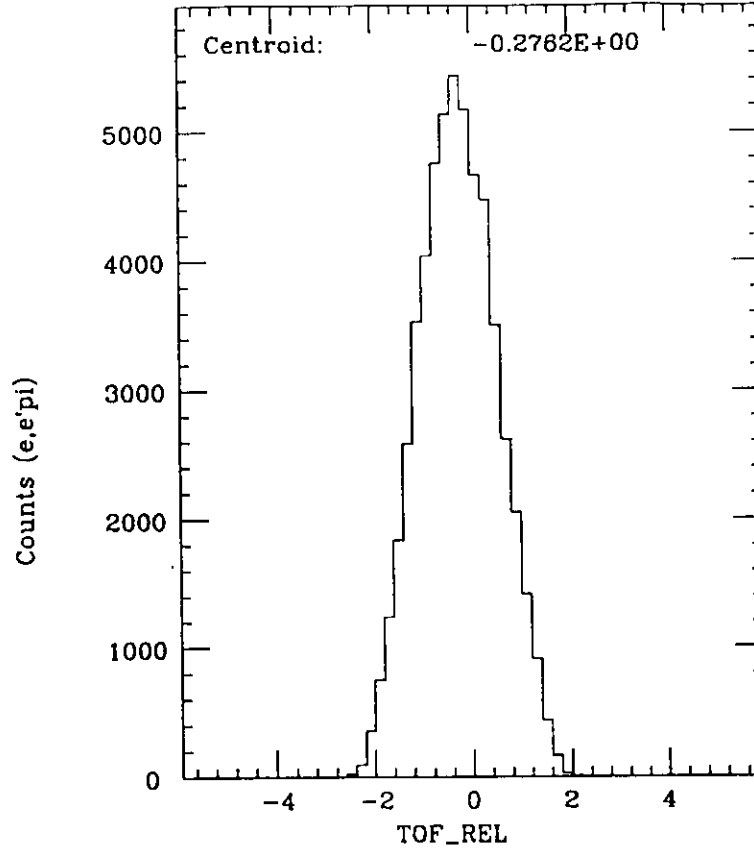


Figure 16. Time of Flight of the Electron Spectrometer relative to the Hadron Spectrometer $TOF_{e'} - TOF_{\pi}$. Even though electrons always have $\beta = 1$, the TOF of the pion can be less than that of the electron due to the large variation in possible pathlengths within each spectrometer.

all valid electron and π^+ coincidences. In the off-line analysis, flightpath and momentum corrections can be made to the relative timing; it is anticipated that a 1 ns relative timing resolution will ultimately be achievable. The accidental rate estimates below are therefore calculated assuming a 1 ns timing window.